

## **2.5D Models Derived from the Magnetic Anomalies Obtained by Upwards Continuation in the Mimbi Area, Southern Cameroon**

**W. Biyiha-Kelaba<sup>1</sup>, T. Ndougsa-Mbarga<sup>2</sup> J.Q. Yene-Atangana<sup>3</sup>  
P. C. Ngoumou<sup>4</sup> and T. C. Tabod<sup>5</sup>**

### **Abstract**

In this study a MATLAB program to interpolate magnetic data using the inverse square distance approach and separate the regional/residual anomalies by the upward continuation method is developed. The application of this technique in combination with the spectral analysis and 2.5D modeling to the aeromagnetic anomaly of the Mimbi area in southern Cameroon has led to a better understanding of the stratification of the deep and near surface structures, which are sources of the observed anomalies. The maps obtained from filtering show that within the magnetic quiet zone, there is a high negative circular elongated anomaly, which seems to represent an intrusion of a magnetic body within the metamorphic rocks of the region.

Two S-N profiles are drawn on the total and residual aeromagnetic anomaly maps respectively. The data sets derived from these profiles made it possible through a program written in MATLAB to have on one hand, the spectra of energy and on other hand, the depths of the sources of observed anomalies. Two 2.5D models of the subsurface structures have been proposed along the profiles P1 and P2, which were drawn on the residual map, obtained after an upward continuation up to 8.3 km. The 2.5D models obtained show a magnetic body, with a signature suggesting two masses close to opposite polarity, which characterize the iron-bearing formations.

**Keywords:** Aeromagnetic data, upward continuation, residual anomaly, spectral analysis, 2.5D modelling, MATLAB, Mimbi area, Cameroon

---

<sup>1</sup>Department of Physics Faculty of Science, University of Yaoundé I, Cameroon.

<sup>2</sup>Department of Physics Advanced Teachers' Training College, University of Yaoundé I, Cameroon .

<sup>3</sup>Department of Earth Sciences, Faculty of Science, University of Yaoundé I, Cameroon.

<sup>4</sup>Department of Physics Faculty of Science, University of Yaoundé I, Cameroon.

<sup>5</sup>Department of Physics Faculty of Science, University of Yaoundé I, Cameroon.

## 1 Introduction

In geophysical exploration during the last decade, potential field methods have a renewed interest in the search for solid mineral and hydrocarbons. In the gravity and magnetic method data processing, the first and the most crucial step is the removal of the effect of deep-seated structures from the observed Bouguer gravity or from the observed total magnetic fields, in order to enhance the signatures of shallow bodies (Ndougsa et al., 2007). These shallow bodies are associated in solid mining exploration firstly to precious metals (gold, diamond) which have a different density with the surroundings (gravity exploration) and secondly to substances such as magnetite, hematite, which have contain an iron ore deposit (magnetic exploration) (Ndougsa et al., 2012).

The Mimbi area is located in the central-south of Cameroon bounded by latitude  $3^{\circ}$  N- $3^{\circ}30'$  N, and longitude  $12^{\circ}$  E- $13^{\circ}$  E (Figs. 1a-b). This area with 650 m average altitude is founded in the southern plateau of Cameroon (Fig.1b) and is made up of a monotonous landscape, mainly of gentle undulating dome shaped hills of convex-like slopes and very few rocky domes with concave slopes (Shandini et al. , 2010). Total magnetic field data measured for geophysical exploration purposes comprise the superposition of the effects of all underground magnetic sources. Usually the targets in archaeological magnetic exploration are small, shallow depth anomalies, and their magnetic field is superimposed to the regional field that comes from larger or deeper sources. The estimation and subtraction of the regional field leads to the residual field that corresponds to the target sources. (Basseka et al, 2011).

The Mimbi area is appertained to the iron belt including south Cameroon, northern Congo and Gabon. Previous geophysical work carried in this region includes aeromagnetic investigation by Paterson et al. (1976).The aim of this study is therefore to use the aeromagnetic data of the Mimbi zone to investigate the major tectonic features and the subsurface geology. The investigation used the combination of some techniques such as spectral analysis based on Fourier transform with the inverse square of distance interpolation, the upward continuation regional-residual separation approach and the 2.5D modelling of residual anomaly.

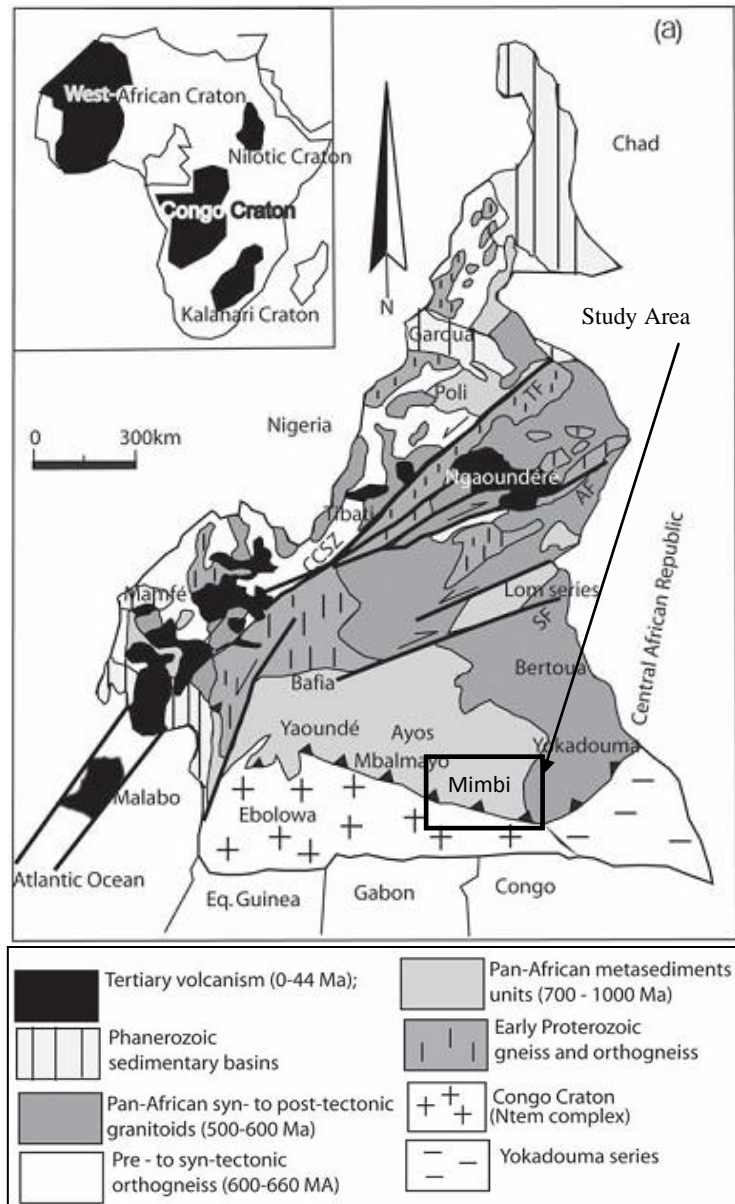


Figure 1: (a) Geological sketch map of Cameroon showing its main lithological units and the location of the Mimbi-Bengbis area.

TF = Tcholliré Fault, AF= Adamaoua Fault, SF = Sanaga Fault  
(Modified after Soba et al.1989, Vicat 1998, and Toteu et al. 2001).

## 2 Geologic and Tectonic Setting

The geology of Mimbi area comprises rocks resulting from the intermediate series, made up of schist and quartzite formed following an epizonal metamorphism (Fig.1b-c). It belongs indeed to the meta-sediments series of Ayos-Mbalmayo-Bengbis, which according to Paterson et al. (1976) is made of pelitic schist identified in Yaounde-Akonolinga axis (Olinga et al., 2010).

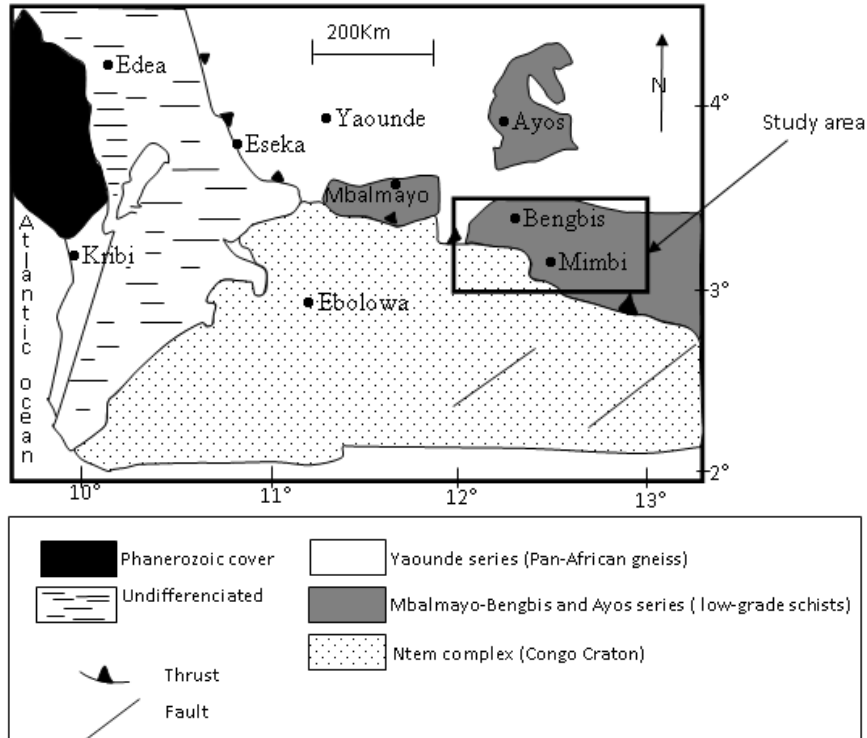


Figure 1: (b) Geological sketch map of Southern Cameroon showing its main lithological units. (Modified after Olinga et al., 2010).

The Bengbis series is mainly composed of schist and quartzite reworked under green schist facies with an E-W belt of about 1500 km (Vicat, 1998).

The composition is made up of chlorite-schist, mica-schist with or without garnet, gneiss and slate with numerous veins of quartzite running through them. The Ayos-Mbalmayo-Bengbis series contains the same metasedimentary composition as the Yaoundé series but the difference is that they were metamorphosed and deformed at different structural levels (Olinga et al., 2010). The Mimbi area is characterized by three main groups of rocks (Fig.1c): banded gneiss and micaschist (mostly semi-pelitic) with interlayered amphibolite, metamorphosed calc-alkaline intrusive rocks and low-grade schists and quartzite. The gneisses are intensively migmatized, as demonstrated by quartzofeldspathic veins, which are running parallel to, or crosscutting the banding of the rocks. The distinguished rock groups have been dated at  $620 \pm 20$  Ma (Penaye et al. 1993; Toteu et al. 2004; Toteu et al. 2006). Detailed descriptions of their chemical characteristics are provided by Nédélec et al. (1986), Nzenti et al. (1988), Ngnotue et al. (2000), Mvondo et al. (2003) and Olinga et al., (2010). They are thought to be derived from iron-rich carbonaceous shales, arenites and greywackes that were intruded by dioritic rocks in either a continental basin or a passive margin environment.

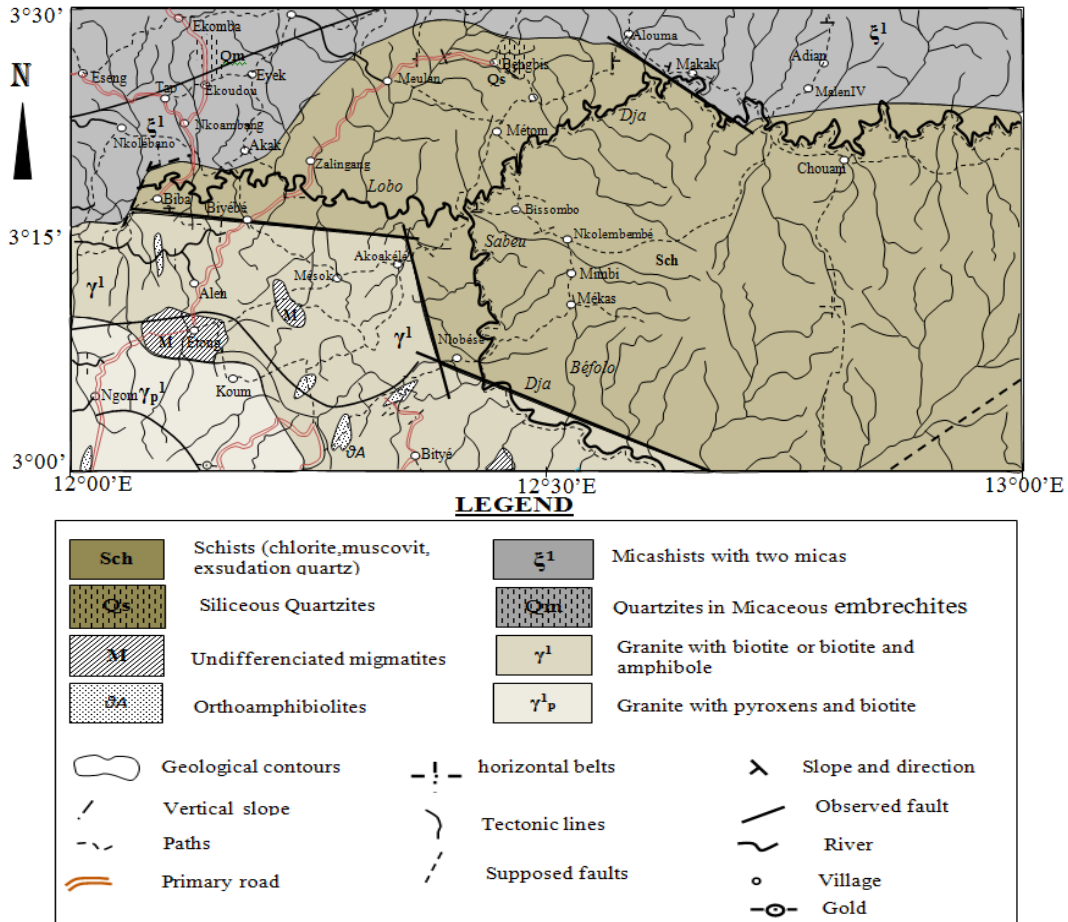


Figure 1: (c) Geological map of Mimbi-Bengbis area (modified after Champetier de Ribes and Aubague, 1956; Guiraudie and Gazel, 1965).

The schists are typically made of a chlorite-muscovite-quartz unit, with tourmaline, zircon and oxide iron like additional minerals (Champetier & Aubague, 1956; Guiraudie & Gazel, 1965). Approximately, in the north of Mimbi, the rocks observed are rolled schists, with biotite, muscovite, and chlorite, containing some quartz grains. We note the absence of intrusive rocks. The schist seems to have been formed from clayey or limestone sediments. The mica-schist of this region is thought to have been formed on top of the chlorite-schist. The primary minerals of the schist include muscovite, biotite, quartz and garnet, disthene, rutile and ilmenite as its secondary minerals (Ndougsa et al., 2003; Paterson et al., 1976). The schist and mica-schist are relatively less faulted. The granites are of the calco-alkalinc and leucocratic type and with enough heterogeneity in its mineralogy.

In a tectonic point of view, it should be noted that the pelitic schists are finely rolled. They are subhorizontal and do not seem to be disturbed by any crumpling. In the north of the zone, they rest in discordance on older schists and gneisses, and in the south they are in contact with granitic rocks by faults (Fig.1c). They seem to be older than the sediments of Dja and their age is probably of the superior Archaean or the inferior Proterozoic. According to the tectonic history, it is thus a stable zone. This zone presents two networks of faults directed respectively NE-SW and NW-SE (Champetier & Aubague, 1956).

### 3 Aeromagnetic Data

The aeromagnetic data in Cameroon was collected over a total surface area of 168.365 km<sup>2</sup> (Paterson et al., 1976). This area was divided into six regions of which the area of study is found within the Bengbis grid. The survey was carried out at a nominal terrain clearance of 235 m which was monitored by a radar altimeter with an accuracy of  $\pm 20$  m. The line spacing of the flight was 750 m but the real distance rarely went above 1 km and the flight direction was N-S.

In the present work, the aeromagnetic anomaly map of Mimbi area lying in the space between latitude 3°00'-3°30' N and longitude 12°15'-12°45'E (Fig.1c) has been re-digitized using the MAPINFO.7.5 package in the near total of the study zone, in order to have an important distribution of data, for a better interpolation. The data collected were then gridded producing a new aeromagnetic anomaly map of contour interval 37 nT plotted (Fig. 2) with the use of our Matlab computer code interpolation based on *Inverse Distance to a Power (IDP)* gridding method.

Based on the total magnetic field anomaly map established by Paterson et al. (1976), 945 data of points named  $f_{mn}$  were re-digitized using Mapinfo 7.5 package. We also realized a 46×60 rectangular grid of points, with a spacing of  $\Delta x = 0.464$  and  $\Delta y = 0.459$ . In each nodes of grid, the data have been calculated using the inverse distance-weighted gridding interpolation. Assuming grid spacing in the frequency domain as  $\Delta u = 0.0468$  and  $\Delta v = 0.0363$ .

## 4 Methods of Analysis

### 4.1 Fourier Transform

The recent developments on Fourier transforms, for interpretation of gravity and magnetic anomalies (Billings et al., 2002) have shown that the Discrete Fourier Transform on scattered data with 2-dimensional approach is given by:

$$F_{jk} = \Delta x \Delta y \sum_{n=1}^N \sum_{m=1}^M f_{mn} \exp(-2\pi i (\frac{jn}{N} + \frac{km}{M})) \quad (1)$$

where  $F_{jk}$  is the Fourier transform for the  $j$ -th row and  $k$ -th column in the frequency domain, of the scattered data  $f_{mn}$  which represents the discrete data array of gravity or magnetic data, for the  $n$ -th row and the  $m$ -th column in the space domain, from  $N \times M$  rectangular grid, with a spacing of  $\Delta x$  and  $\Delta y$ ;

$i^2 = -1$  is a complex number. Thus starting from  $F_{jk}$ , we deduce  $f_{mn}$  by inverse discrete Fourier transform, assuming grid spacing in the frequency domain  $\Delta u$  and  $\Delta v$  :

$$f_{mn} = \Delta u \Delta v \sum_{j=1}^{N/2} \sum_{k=1}^{M/2} F_{jk} \exp(2\pi i (\frac{jn}{N} + \frac{km}{M})) \quad (2)$$

As the data spacing  $\Delta x$  and  $\Delta y$  is approximately constant, an upper limit on frequencies resolved by the data can be estimated by the Nyquist relationship,  $u_{max} = 1/(2 \Delta x)$  and  $v_{max} = 1/(2 \Delta y)$ . Any higher frequencies that are present in the signal are aliased into the Nyquist limits.

The Fourier transformations are used extensively in the processing of geophysical data (Billings et al., 2002). They are required, among other things, to calculate the depth to basement from airborne magnetic surveys (Blakely, 1995), to downward and upward continue magnetic surveys (Henderson and Zietz, 1949), to calculate components of

potential field in specified directions, in reduction to pole for magnetic survey (Ervin, 1976).

The algorithms of fast Fourier transform (FFT) were developed by Gentleman and Sande (1966) in order to reduce the maximum computing times. These algorithms are applied for the study of gravimetric and magnetic anomalies, by means of the processes of sampling.

The transformed map in fact are obtained by controlled procedure of Fourier, who allows to realize at the same time, independently, two kinds of operations: on the one hand separation by frequential cut of part of the data, according to whether those require it or allow it; and in addition the vertical transformation, by derivation or prolongation of the data selected (Gerard and Griveau, 1972).

## 4.2 Spectral Analysis

Spectral analysis is a quantitative method, based on the properties of the energy spectrum of large and complex aeromagnetic or gravity data sets. It uses the 2-D Fast Fourier Transform and transform magnetic or gravity data from space domain to frequency domain. It makes it possible to consider the depths average of the bodies disturbing, sources of anomalies.

This method was used by several authors (Spector and Grant, 1970; Gerard & Debeglia, 1975; Bhattacharya and Leu, 1975 and 1977; Njandjock et al., 2006) for the estimation of average depths of the magnetic or gravimetric sources bodies. Pal et al., (1978) evoke that the transformation of Fourier of the gravimetric and magnetic anomalies of space to the frequential field, produces a method right for the estimate depth of the sources, when these sources are indicated by weak components of frequencies of the anomaly.

The power spectrum function is transformed mathematically by technique of Fourier and the logarithm of the power contained in each frequency of the field that the sources create at a distance  $h$ , decreases linearly with increasing frequency within discrete segments of the spectrum (Tadjou et al., 2009).

Thus, the depth  $h$  of the roof of the body can be estimated by the formula below:

$$h = \frac{\Delta \text{Log}(E)}{4\pi(f)} \quad [\text{Gérard \& Griveau, 1972}] \quad (3)$$

where  $E(f) = e^{-2hf} = |F(f)|^2$  is the energy spectrum (the square of the Fourier amplitude spectrum) and  $\Delta \text{Log}(E)$  is the variation of the logarithm of the power spectrum in the interval of frequency  $\Delta(f)$ .

The energy spectrum generally has two sources. The deeper source is manifested in the smaller wavenumber end of the spectrum, while the shallower ensemble manifests itself in the larger wavenumber end. The tail of the spectrum is a consequence of high wavenumber noise (Tadjou et al., 2009).

## 4.3 Upward Continuation

The upward continuation is a residual and regional anomaly separation method, that one subjects the observed potential field (gravimetric or magnetic) on a surface, in order to obtain the field which would be observed on another surface above (according to upwards continuation) or in lower part (according to downwards continuation) of the initial surface observation (Blakely, 1996). Another approach was proposed by Jacobsen (1987).

According to Jacobsen (1987) upward continuation was chosen as a means of extracting the residual gravity field for the transformation to be possible, and the fields of potentials must vary in a continuous way with a distance from the source, with the interior of any area of space not containing the source of the field (Anecchione, 2001). In the space domain, the upward continuation is described by the integral as follow:

$$U(x, y, z_0 - \Delta z) = \frac{\Delta z}{2\pi} \iint_{-\infty}^{+\infty} \frac{U(x', y', z_0)}{[(x-x')^2 + (y-y')^2 + \Delta z^2]^{3/2}} dx' dy' \quad , \quad \Delta z > 0 \quad (4)$$

$U$  is the gravity or magnetic potential field;  $z_0$  is the initial observation plan.  $\Delta z$  is the continuation distance. Vertical distance  $Z$  is positive downwards. The transformation becomes a simple multiplication in the Fourier domain:

$$F[U_p] = e^{-2\pi\Delta z\sqrt{u^2+v^2}} \times F[U] \quad (5)$$

$F$  represents the Fourier transform.  $U_p$  is the field prolonged upwards with  $u$  and  $v$  frequencies of the signal source. The factor  $e^{-2\pi\Delta zX}$  is the upward continuation operator. The effect of the operator is to attenuate the amplitudes of the components of the field according to their increasing wavenumber. For the raised wavenumber, the operator tends towards zero, and ends in an important reduction of the amplitude of the components of the field of short wavelength (Blakely, 1996). The filter attenuates amplitude at smaller wavenumber with respect to those at greater wavenumber. The result is a map poorer in smaller wavenumbers compared with the total field anomaly (Anecchione, 2001).

Upward continuation is a smooth filter attenuating amplitude progressively with increasing wavenumber. The upward continuation is also characterised as a powerful low-pass filter, because the low or weak frequencies are priority, those high are simply cut. The residual is defined as the subtraction of the upward continued total field anomaly from the total field anomaly.

It is enough to calculate the inverse Fourier transform to obtain the prolonged field. The upward continuation expresses regional structural directions. The technique of residual-regional separation based on an upward continuation of the anomaly is connected to the immediate effect of the distance between the sources and the plan of measurement. Since the distance increases upward, the signals of the surface sources are attenuated. What we see is the field produced by the major sources, therefore regional (Anecchione, 2001).

#### 4.4 Inverse Square Distance Interpolation

The algorithm of separation of the anomalies is based on the formula (1) and (5) suggested by Billings et al. (2002) and Blakely (1996) respectively for the Fourier transforms, and the upward continuation operator. The algorithm initially consists of creating an irregular or regular grid of points. The data will be introduced starting from an Excel file data. In the second situation, the program carries out an interpolation of the data in the grid thus generated. The method of interpolation used in this work is the inverse distance-weighted gridding method. Franke (1982) assumes that, the inverse distance to a power gridding method (IDPGM) is a weighted average interpolator, and can be either an exact or a smoothing interpolator. With the IDPGM, data sets are weighted during interpolation such that the influence of one point relative to another declines with distance from the grid node. Weighting is assigned to data through the use of a weighting power that controls how the weighting factors drop off as distance from a grid node increases.

The greater the weighting power is, the less effect points far from the grid node have during interpolation. As the power increases, the grid node value approaches the value of the nearest point. For a smaller power, the weights are more evenly distributed among the neighboring data points.

The general form of the anomaly estimated in a node M is given by the following expression:

$$Z_j^* = \frac{\sum_{i=1}^n \frac{1}{h_{ij}^\beta} Z_i}{\sum_{i=1}^n \frac{1}{h_{ij}^\beta}} \quad \text{with } h_{ij} = \sqrt{d_{ij}^2 + \delta^2} \quad (6)$$

Where  $h_{ij}$  represents the separation distance between the grid node j and neighboring point i.

$Z_j^*$  is the interpolated value of the anomaly for grid node j.

$Z_i$  are the neighboring points,  $\delta$  represents the smoothing parameter and  $\beta$  is the weighting power.

#### 4.5 Map Analysis

In general, the total magnetic field anomaly reflects a superposition of regional and residual components. In order to analyze the contribution of the various shallow components present in the data, it is necessary to separate them. To constrain the separation of the local and shallower components (residual anomaly) a good understanding of the geological and tectonic context of the study area is very helpful. The choice of regional-residual separation technique is also a key point (Agocs, 1951; Simpson, 1954; Thurston and Brown, 1992; Beltrao et al., 1991; Ndougusa et al., 2007).

Generally, during the separation of the total magnetic field anomaly (or Bouguer anomaly) into individual anomalies, there are essentially two steps:

- the estimation of the regional anomaly (reg);
- the subtraction of the regional anomaly from the total magnetic field anomaly (or Bouguer anomaly) to obtain the residual anomaly (res).

The regional anomaly has been deduced based on the upward continuation approach by the following expression (Blakely 1996)

$$\text{Re } g(n, m) = \text{real}[\Delta u \Delta v \times \exp(2\pi i(\frac{jn}{N} + \frac{km}{M})) \times F[U] ] \quad (7)$$

and the residual anomaly has been calculated from the following formula:

$$\text{Re } s(n, m) = U(n, m) - \text{Re } g(n, m) \quad (8)$$

The magnetic units have been identified by using the approach developed by many authors (Paterson et al., 1976; Prieto, 1996; Wong & Laughlin, 1998) which is based on the anomaly characteristics. The criteria are:

- ✓ Mean anomalies amplitude;
- ✓ The polarity of the anomaly;
- ✓ The shape and the patterns of the anomaly contours;

The length of the profile is chosen in order to minimize the edge effect on the modeling.

## 5 Results

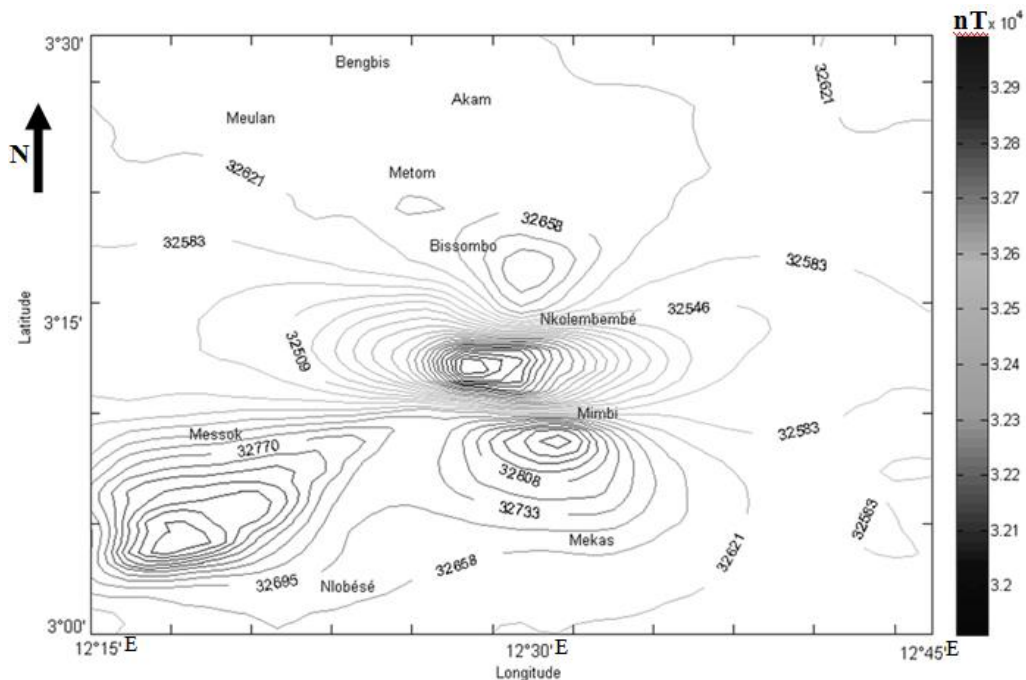
### 5.1 Analysis of the Aeromagnetic Total Field Map

The aeromagnetic anomaly map of the total field (Fig.2) was obtained from the inverse square distance-weighted gridding interpolation code. The suitable smoothing parameter to have smooth contours was  $\delta = 0.6$ . The resulting aeromagnetic anomalies were then plotted to obtain an anomaly map (Fig.2) with contours at 37 nT interval. This map is broadly similar to those reported by Paterson et al. (1976).

The analysis of this aeromagnetic map permitted to divide it into magnetic sectors of high, moderates and low magnetic intensity. It is overall characterized by anomaly values ranging from about 32000 to 33000 gammas. The area under study presents a complex magnetic response.

The circular elongated anomalies with the E-W trend are smoothed magnetic anomaly zone, and they are characterized by low values of the magnetic intensity.

They are found around Nkolembembé. In this part of the area, the magnetic response varies from 32000 to 32500 gammas. The strongly attenuated magnetic signal that covers the schists of the region, is probably corresponds to rocks which have a tiny content of magnetite, and consequently contain less ferromagnetic materials. This elongated anomaly can be correlated to an intrusion within the basement.



The zones of complex or strong anomalies are overall in the southern part of the study zone towards Mimbi, where the magnetic trends are oriented in the NE-SW direction. They are also identified in the south-western part towards Messok where isomagnetic contours present a SW-NE direction, and finally in the North of the area of study, around Bissombo where they are directed N-S. Broadly one records the strongest magnetic intensity varying from 32800 to 33200 gammas. As a general point of consideration, the circular form of observed isomagnetics contours suggests an intrusion of a magnetic body to a great depth or an average depth around the meta-sediments (schist) met in almost all the zone. In addition, the circular anomalies of Nkolembembé and that of Mimbi make us think to a bipolar magnetic body spread out in layer along this zone. It is however difficult to correlate the observed magnetic anomalies with the geology of the study area.

## 5.2 Spectral Analysis on Total Field

A quantitative interpretation of aeromagnetic anomalies was done using spectral analysis over the entire area. Two plots of log average power spectrum versus wavenumber for the magnetic field over the region were derived from the magnetic signatures (Fig.4) to determine the depth of the deep anomalous sources.

Two profiles P1 and P2 were respectively chosen and drawn on the aeromagnetic total field map (Fig.3). These profiles were drawn with a North-South orientation and traversing through the circular isomagnetics contours observed around the study area.

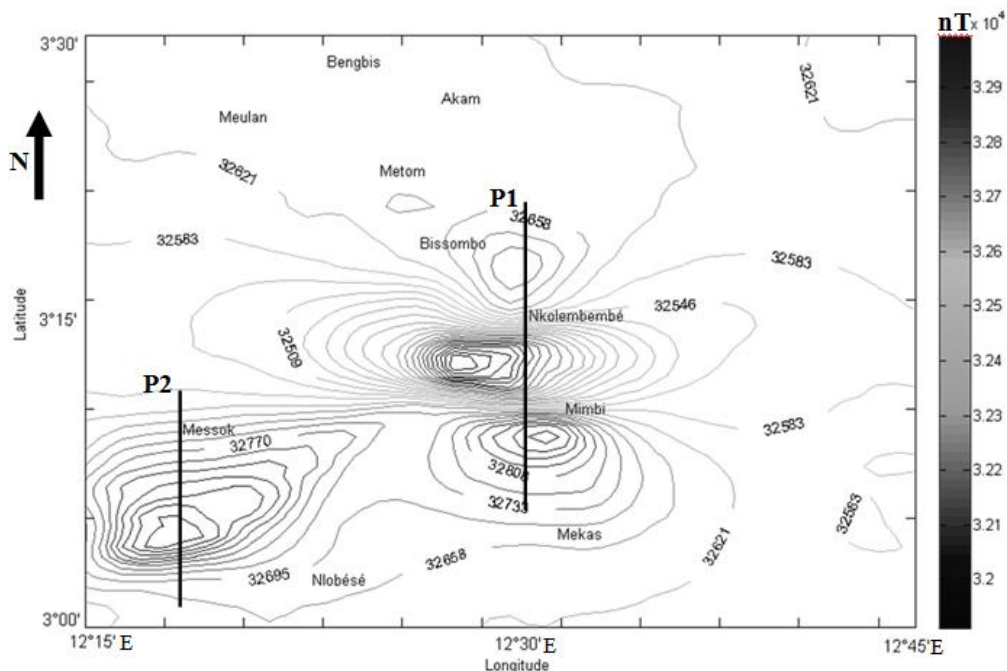


Figure 3: Aeromagnetic total field map with profiles for spectral analyses.

The profile P1 has its origin at latitude 3°05' N and lies parallel on longitude 12°30' E up to latitude 3°17' N and crosses the villages of Bissombo and Mimbi. This profile passes through the schist formations from the south to the north of the geological map. Along the profile, we have three regions of high positive anomalies that create a high gradient with the strong anomalies around Bissombo and Mimbi areas and smooth anomalies around

Nkolembembé. This gradient zone and other traced zones along the profile are the areas of interest. There is also a highly suspected zone of an intrusion about 3°15' N around Nkolembembé, because this part is characterized by a high negative anomaly that occurs between two positive anomalies.

The profile P2 runs from latitude 3°02' to 3°12' N. It lies parallel along longitude 12°17'E. The profile cuts across Messok (Fig.3). From the south, the profile cuts through the granites and lastly the schist at the north of the region. Along the profile, we have a region of high positive anomalies that create a high gradient with the positive anomalies around Messok.

The curves of power spectrum obtained from the profiles (Fig.4), give the regional and residual depths (Hreg and Hres respectively), as Table 1 indicates it. These depths (Table 1) of the anomaly sources were calculated from plots of the log of the energy spectrum versus the wavenumber of the aeromagnetic total field anomalies.

Table 1: Depth obtains from spectral analysis on magnetic total field map.

Profile	Hreg (km)	Hres (km)
<b>Bissombo-Mekas (P1)</b>	8.2 ± 0.4	2.1 ± 0.1
<b>Messok (P2)</b>	8.4 ± 0.4	0.0140 ± 0.0007

The depths obtained from the slope of the curve represent the average depth of the top of the anomaly sources. The calculation of the error for the depths was also included in the computer code by following the approach developed by Nnangue et al. (2000). The mean least square method and taking into consideration that the error should be at most 10% of the depth were implemented for the calculation. The regional depths represent the far away or deeper sources which are considered as anomaly sources. These are long wavelength sources. The residual anomaly depths serve as one of the constraints for the modelling that follows (Ndougsa et al., 2011).

The major sources are magnetic bodies located at depths varying between 8.15 km and 8.43 km. The 2.05 km and 0.014 km depths were associated with intermediate magnetic layers in discordance with the surface rocks of the zone. The regional depths represent the far away or deeper sources which are considered as anomaly sources. These are long wavelength sources. The residual anomaly depths serve as one of the constraints for the modelling that follows. An average of 8.3 km of the regional sources will be adopted in order to carry out an upward continuation of the total aeromagnetic field, which expresses regional structural trends. The difference in residual depth between the two profiles P1 and P2 would translate the existence of a strong dip of the magnetic bodies resulting from the crust; dip which would extend from Messok to Mimbi. Moreover, it would translate an unevenness which puts forward a structure faulted between Messok and Nkolembembe.

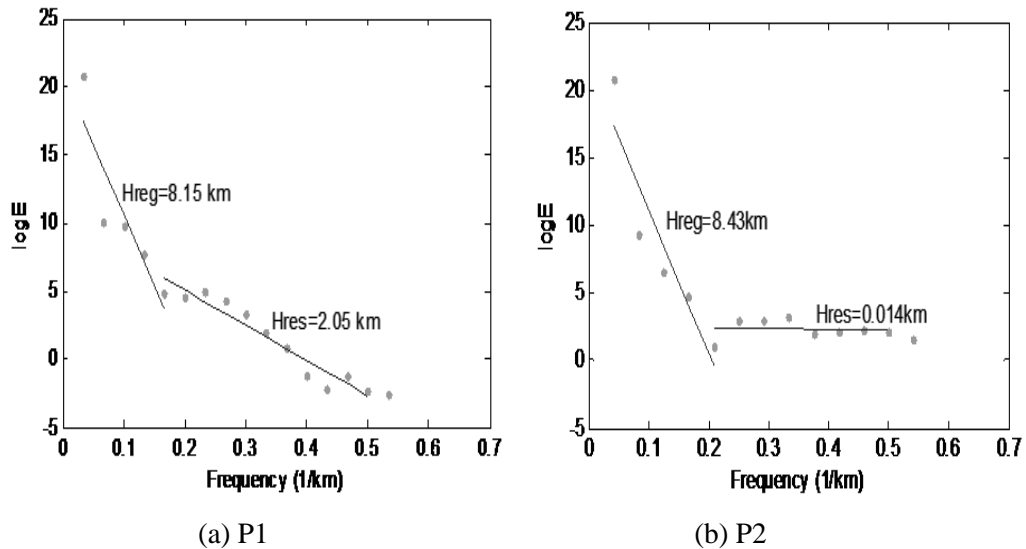


Figure 4: Power spectrum curves of the total field profiles.

### 5.3 Analysis of the Regional Map

The map prolonged upward (Fig. 5), makes it possible to highlight the great wavelengths anomalies. The form and the extension of the anomalies are function of the continuation distance. The regional anomalies map (Fig. 6) with high wavelengths amplitudes ranging from 32614 to 32626 gammas, shows closed isomagnetic contours at Nkolembembé and Messok. This suggests that the anomalies observed on the total magnetic field map are the manifestations of lower deeper magnetic bodies and makes us think that we have either a deeper intrusive magnetic bodies at these places, or a less magnetic intrusive body founding at average depths of about 8 km such as we have proposed in regional spectral analysis on total field. This regional pattern also suggests a thinning of the crust. In lower part of the circular anomaly of Nkolembembé and in the North of the study zone, covering the villages of Bissombo, Akam, and surroundings, the long and linear pattern of isomagnetics contours suggests a faulted alignment at surface, because of the non-closed of anomalies with a W-E global direction.

### 5.4 Analysis of the Residual Map

The observations made on aeromagnetic total field anomalies map, are more visible on residual aeromagnetic anomaly map (Fig.6). Indeed the subtraction of the regional component to that of the total field, leads to the residual map, which helps with better understanding the response of the structures and the surface litho-logical units.

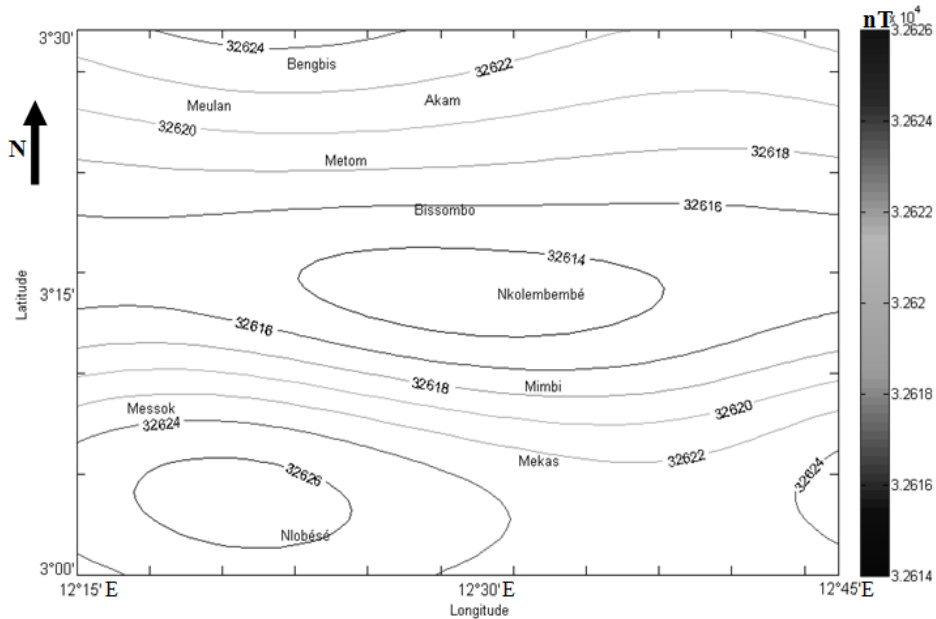


Figure 5: Regional anomaly map obtained by upward continuation up to 8.3km (Contour interval=2, unit=gamma).

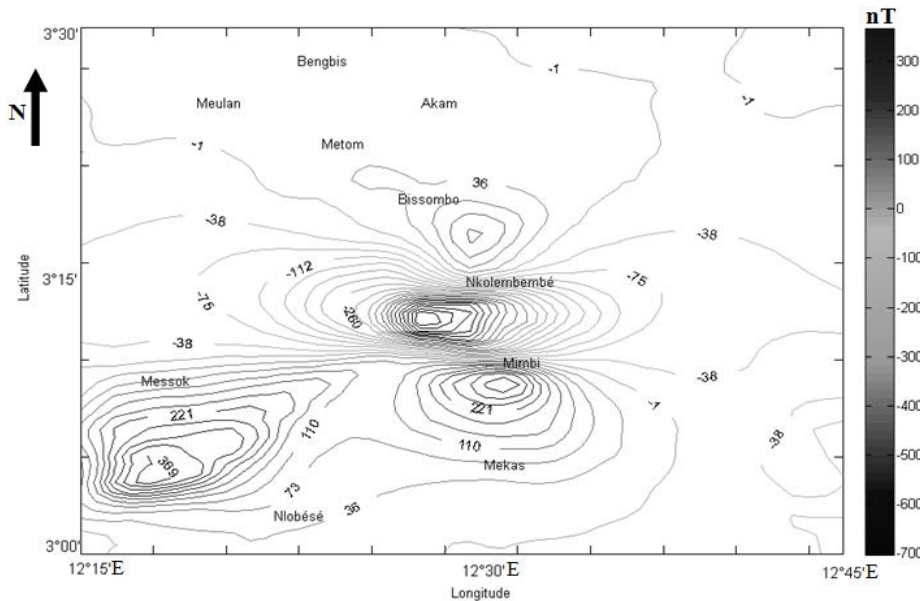


Figure 6: Residual anomaly map (interline=37, unit=gamma).

This residual map keeps the same form of contours as total field map and matches more clearly the relative intensities of the levels of the magnetic activity as well as the direction of isomagnetic contours in different zones of the map. The localized anomalies (or related to relatively sources surface) are strongly put forward with a short wavelengths amplitude of anomalies ranging from -700 to +300 gamma(nT), bounded between 3° N to 3°30' N in latitudes and 12°15' E to 12°45' E in longitudes. The values indicated by the residual express on one side, the variations of susceptibility of the surface magnetic bodies which must be directly related to the side variations of the geological units. We

have for a detailed or qualitative study, delimited the study area via the residual aeromagnetic map in magnetic units (Fig.7) presenting different magnetic characteristics (the average amplitude of the anomalies, dominant polarity of the anomalies, the shape of the profiles of the anomalies, the lengths of the contour patterns of anomalies).

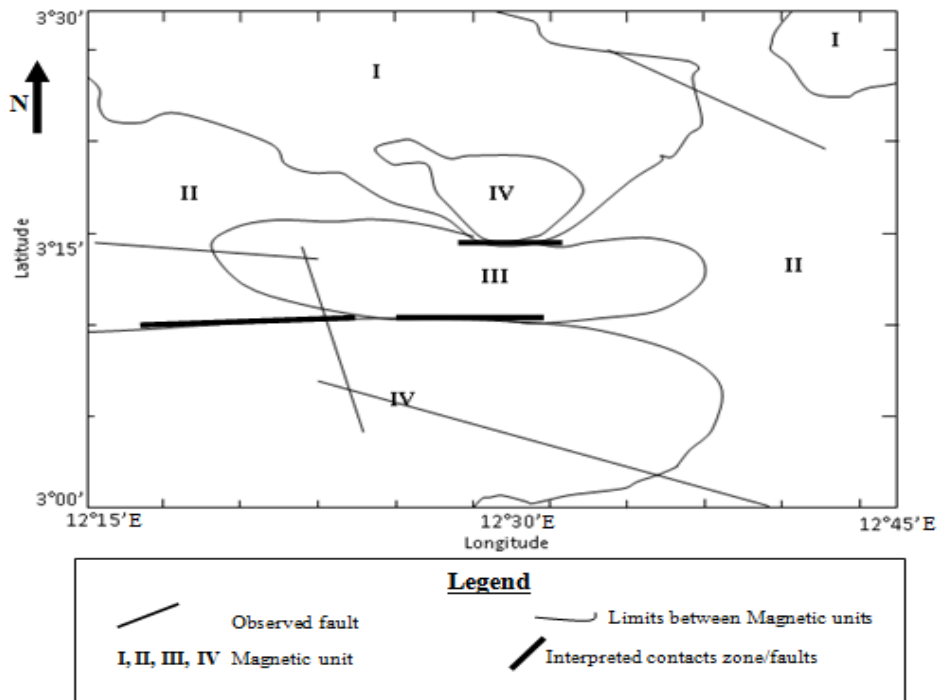


Figure 7: Magnetic units map.

### ***Unit I***

It is characterized primarily by an attenuated magnetic response and consequently corresponds to rocks on the surface, which have only one tiny content of magnetite. The magnetic disturbances emanating from the surface rocks are positive anomalies ranging from +10 to +30 gammas. These rocks contain less ferromagnesian materials and can be correlated to less magnetic schists. Unit I is located in the far North-West, and covers the North-eastern part of the study zone, containing Meulan, Akam, Metom and Bengbis villages.

### ***Unit II***

It presents attenuated negative magnetic response, whose average of amplitude is around -38 gamma and corresponds to rocks whose contain negligible or null magnetite amount. It covers the South-eastern part and. would be spreaded out in the form of vertical corridor towards the North-East. In addition, it also accentuated towards the West of the Nkolembembé area, along the central corridor of horizontal axis, around 3°15'. This unit is not basically magnetic.

### ***Unit III***

Unit III is goshawks of Nkolembembé overall where the magnetic anomalies with circular owners or closed isomagnetics contours of direction W-E are strongly negative. The observed anomaly amplitude ranging from -100 to -700 gammas. This weak magnetic response is interpreted as an intrusion of less granitic magnetic rocks beneath magnetic

schist and vice versa. Let us recall that these negative anomalies are quasi similar to the structures described by Boukeke (1994) along the RCA (Central African Republic), whose patterns are assumed as magnetizing induced in the rocks having a high magnetic susceptibility.

#### **Unit IV**

This unit gathers the strongest magnetic anomalies of the study zone. It is characterized by three prominent positive anomalies with amplitudes ranging from +100 and +400 gammas. The isomagnetic contours patterns of this unit are especially rounded, elliptic or closed. One of the anomalies goshawks of Messok, precisely in southern part of Messok presents a SW-NE direction. This zone provides an exceptional magnetism above the background noise where the highest intensity is recorded (maximum = 369gammas). The second anomaly zone between Mimbi and Mekas has a NW-SE direction and a maximum intensity of 332 gammas and finally that of Bissombo presents an N-S orientation with maximum amplitude of 147gammas. Those forms of the anomalies seem to indicate sources to thin or tabular layers and are comparable with iron-bearing formations or métasédiments rich in iron. The disposition and edge shape boundaries indicate intrusive nature into the schist terrains. The magnetic variation of amplitude between unit III (Nkolembembé) and unit IV of Mimbi is interesting and seems to correspond to a particular geological feature. Indeed, the magnetic anomaly varies from the negative one with positive in an abrupt way (opposite polarity) with an intermediate zone presenting a zero gradient.

This cleavage seems to materialize the contact or a discontinuity zone between the schists confirmed on the geological map and granite intrusion with pyroxene in the crust. A network of faults is also considered. Units III and IV made after an object of more detailed quantitative study.

#### **5.5 Spectral Analysis on Residual Map**

The spectral analysis (Fig.9a-b) carried out on the residual map starting from the profiles P1 and P2 (Fig.8), enables us to constraints the 2.5D modeling by bringing in a righter and significant manner, to estimate depth of the bodies (Table 2) resulting from the shallower crust, which are the sources of the observed anomalies.

Table 2: Depth obtains from spectral analysis on magnetic residual map.

<b>Residual profile</b>	<b>Hres1 (km)</b>	<b>Hres2 (km)</b>
<b>Bissombo-Mekas (P1)</b>	2,5 ± 0.1	1.37 ± 0.07
<b>Messok (P2)</b>	3,4 ± 0.2	0.77 ± 0.04

The first depth (Hres1) of about 2.46 km for P1 and 3.36 km for P2 represents the higher depth of the roof of the magnetic body, while the depth (Hres2) identified to be 1.37 km for P1 and 0.77 km for P2 shows the lower limit of the magnetic body. It corresponds to the anomalies identified along the axis Bissombo-Nkolembembé-Mimbi and towards Messok respectively. In short, these heights would translate overall, the interval in which the magnetic bodies suspected in the concerned zones would be located. The values of depth obtained from the spectral analysis are used as constraints for the subsurface model.

## 5.6 2.5D Modelling

Many authors' (Grant & Martin, 1966; Gérard & Griveau, 1972; Prieto, 1996) have quantitatively interpreted magnetic or aeromagnetic anomalies. In the present study, we combined within the framework of the quantitative analysis two methods: spectral analysis and 2.5D modeling. The depths obtained from the spectral analysis were used as constraints of the model depths, and the 2.5D models are done following Cooper (2003) approach. This approach is based on Talwani (1965) type algorithm to calculate the anomaly. The geomagnetic field, the inclination and the declination of the region, the bearing of the profile and the reference height at which the data was collected are used as input. The values of the anomalies and the distances obtained from the respective intersections of the profile and the contour lines are also introduced.

We have specified the magnetic susceptibility, the depth of the roof of the structure, the thickness, the transverse extension and the vertical extension following Shuey and Pasquale (1973). The magnetic susceptibility of the various rock types is obtained from Paterson et al. (1976), and compared to those from the literature (Telford et al., 1990). The amplitude of the anomalies depends on the depth and on magnetic susceptibility (Prieto, 1996).

For quantitative analysis of the observed anomalies, we traced two magnetic profiles P1 and P2 (Fig. 8). These profiles directed N-S were selected in the zones of interest where the anomalies are tightened more and of ellipsoidal form. The superimposition of these profiles to the geological map shows that, they over crossed from the South to North: schist for (P1), schist and granite for (P2). For the modeling we assumed the fact that the amplitude's the anomaly depends on the depth and on the magnetic susceptibility (Prieto, 1996).

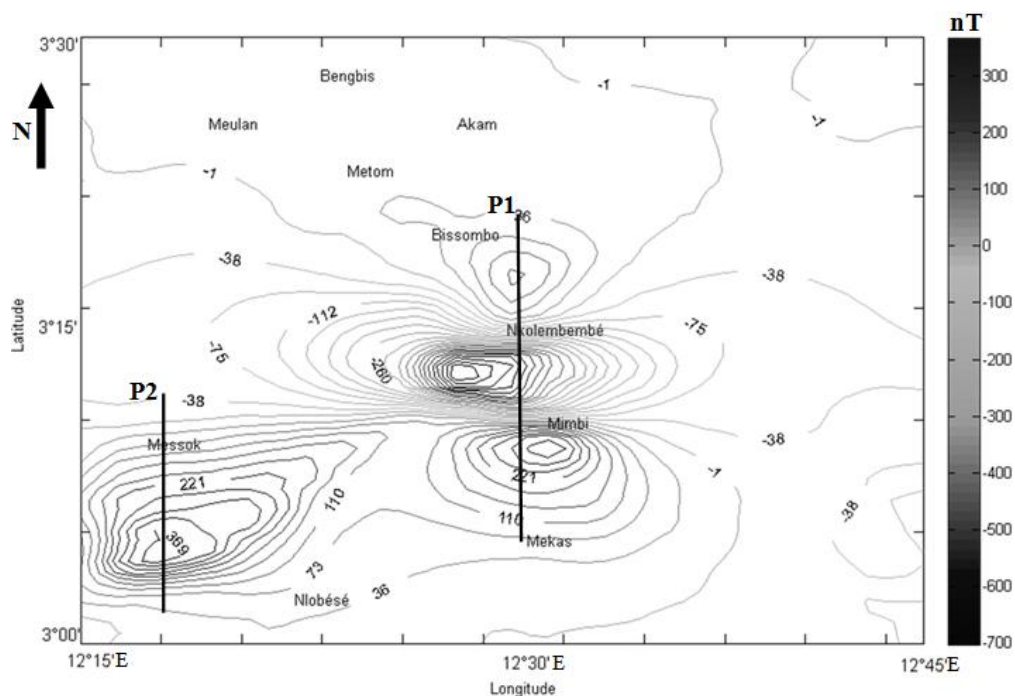


Figure 8: Residual anomaly map and interpreted profiles (Interline=37; unit=gamma).

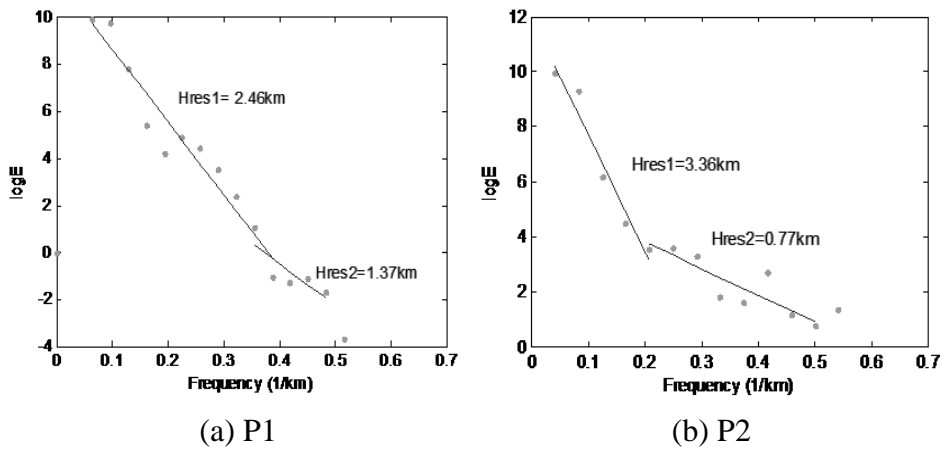


Figure 9: Power spectrum curves of residual profiles

### Profile 1

Profile P1 is covering the axis Bissombo-Mimbi. The cause of the anomaly of Bissombo-Mimbi seems to be from three magnetic bodies of contrary polarity and boxed in the pelitic schist (Fig. 10).

*Bodies 1 and 3, of susceptibility -0.003 (system CGS) would be of opposite polarity and the other body 2, of susceptibility 0.0088 (system CGS) would be of normal polarity. This opposition of polarity observed is a characteristic of the iron-bearing formations which is found in South-Cameroun precisely in Ebolowa-Djoum (Ndougsa et al., 2012; SRK, 2011; Suh et al, 2009).*

The model consists of a unit of rocks presenting the different magnetic characteristics, correlable with massive hematite and itabirite, and being all inside the crust without outcrop on the surface. South in north, we identified the schist formations, in discordances with the granite formations which constitute the basement of zone. The granite intrusion observed separates the two iron-bearing formations boxed in the schists, which would translate a métamorpho-plutonic contact reasonably. This intrusion would probably result from a recrystallization of the magma in the zone; magma coming from the lithosphere where the temperature and the pressure would be raised and which would have migrated through cracks created to this place. We thus have there a contact schist-granite and it should be noted that this contact seems to have created a network of faults in the area. This network of faults follows the direction of the faults observed (Fig.7). These contacts are to approximately 10.6 km and 15.6 km respectively on the basis of the south in the north of the profile. The parameters of these magnetic bodies boxed in the formations of schists, granites and schists respectively, are consigned in Table 3.

Table 3: Geometrics parameters of magnetic bodies, model of P1 profile.

Profile P1 : Bissombo-Mimbi anomalies					
	Susceptibility (CGS unit)	Depth (km)	Width (km)	transversal extension (Strike length) (km)	vertical extension (km)
<b>Body 1</b>	-0.0039	0.26	6.4	50	3
<b>Body 2</b>	-0.0088	0.52	2.9	50	3.5
<b>Body 3</b>	-0.003	0.7	2.3	50	3.5

**Profile2**

The P2 profile covering the zone of Messok presents only one maximum of 402 nT to approximately 4.4 km on the basis of the South. The model (Fig.11) obtained starting from this profile, brings out two magnetic bodies.

Respective bodies 1 and 2 of susceptibility  $-0.0088$  and  $-0.0057$  (system CGS) are of opposite polarity and were identified as iron-bearing formations boxed in schist and granite, the plutonic and metamorphic rocks respectively, and of which the surface structure is lenticular (Paterson et al., 1976). The geological map clearly reveals to us the presence of granite around Messok and localised schists above this zone. It is thus has correlation between geology and the magnetic anomalies observed. These two magnetic bodies would be responsible for the positive anomaly around Messok. However the abrupt variation of unceasingly decreasing anomaly confirms the contact granite-schist observed to approximately 5.4 km on the basis of the south of the profile. This contact or discontinuity is much more visible on the surfaces of some of the geological map and represents the fault located with the top of Messok. These faults are less deep in the crust. In addition, parameters of the two magnetic bodies boxed in the schist and granite formations respectively, and persons in charge of the anomaly of Messok, seen through the P2 profile, are consigned in Table 4.

Table 4: Geometrics parameters of magnetic bodies, model of P2 profile.

Profile P2 : Messok anomaly					
	Susceptibility (CGS unit)	Depth (km)	Width (km)	transversal extension (Strike length) (km)	vertical extension (km)
<b>Body 1</b>	-0.0088	0.79	1.72	10	3.5
<b>Body 2</b>	-0.0057	1.14	5.2	10	3.5

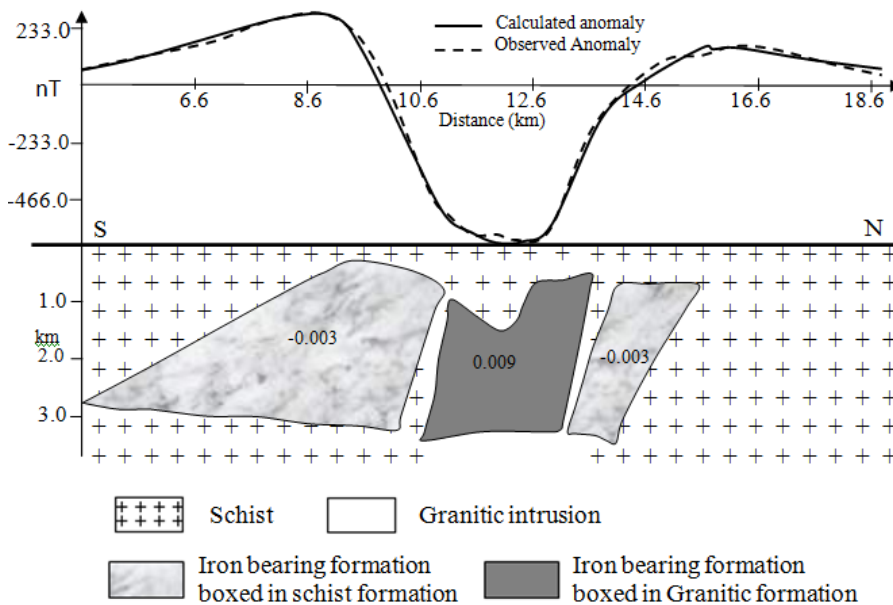


Figure 10: Bissombo-Mimbi anomaly, 2.5D model of profile P1

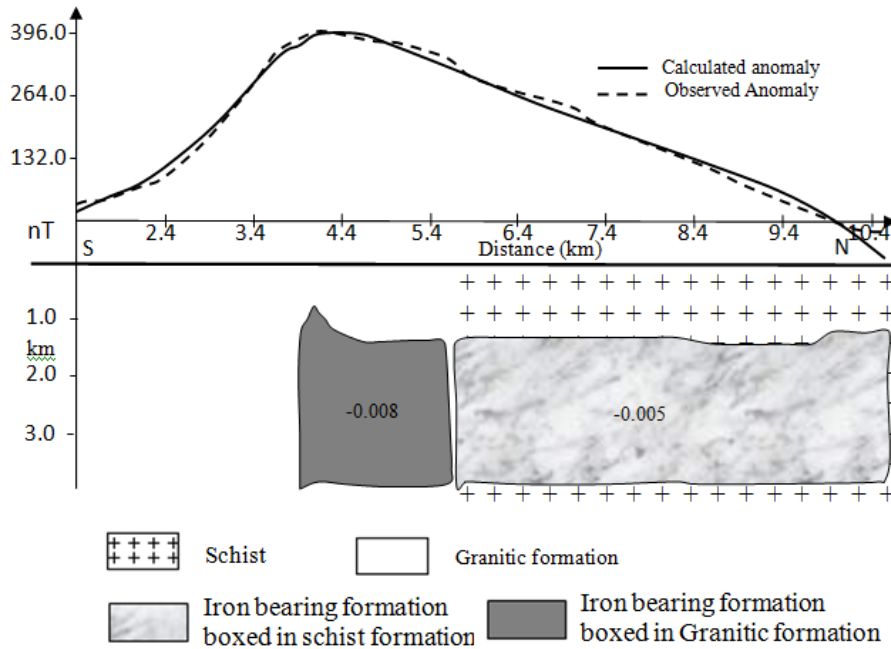


Figure 11: Messok anomaly, 2.5D model of profile P2.

## 6 Discussion

The results obtained during magnetic interpretation are tributary on the one hand, with the technique used for the data processing and on the other hand, with the constraints brought in the choice of the physical parameters intervening in the development of the models. The magnetic lifting will detect only magnetic minerals related to iron. The latter contain very small group of titanium and iron oxides, in which the iron ore (reduced) plays a part dominating. The geological interpretation of the magnetic surveys is closely related on the geology and the geochemistry of magnetite. However, an analysis of the aeromagnetic data cannot make more than to map the distribution of magnetite in base (Paterson et al., 1976). Thus, the total field aeromagnetic anomaly map (Fig.2) makes it possible to better visualize the zones favorable with the ore layers. The residual magnetic anomaly obtained (Fig.6) is supposed to represent the answer of the surface levels insofar as the anomaly of the total magnetic field prolonged to the top represents the answer of the major levels. The spectrum number of wave of the residual anomaly is all the more high as the low-pass filtering of the operator of prolongation to the top is widened towards the high numbers of waves.

The depths of magnetic bodies to minor crustal in the Mimbi area are estimated using spectral analysis of total aeromagnetic anomalies with our computation algorithm. Spectral analysis of magnetic data indicates that the high frequency residual anomalies are of shallow origin. These allow the mean depth magnetic bodies in the region to be evaluated. There are significant changes in the character of the spectrum when one moves from deeper to shallower sources. According to the results obtained in our study precisely in the aeromagnetic total field map, the major sources are magnetic bodies located at depths varying from 8.15 km beneath Messok in the west to 8.43 km along the axis Bissombo Mimbi in the centre of the region. The depths of 2.05 km and 0.014 km obtained from the total field map correspond to the intermediate magnetic layers in

discordance with the surface rocks of the zone. The magnitude of the magnetic gradients analyze as strong end circular anomalies observed in the west of the study area toward messok, in the central vertical axis along Bissombo to Mekas correlate well with the 8.15km-2.05km firstly and 8.43km-0.014km depth secondly and is probably a result of an intrusion of magnetic bodies in discordance with granite, schist formation. This intrusion must have caused the subsidence of the basement along the northern border of the craton (Tadjou et al., 2009). The reactivation of large-scale basement faults would have favoured the upward flow of magma to produce the elongate intrusion identified with circular shape of anomalies in the study area. Two selected profiles (Figs. 10 and 11), trending approximately perpendicular to both the residual magnetic contours and the geological structures, were modeled using the Magdc computer program (Cooper, 2003).

Interpretation of these profiles has shown that the structures responsible for the negative and positive anomalies in the area are three bodies present opposite polarities inside the crust within schist belt formation, according to the first profile, and two magnetic bodies of opposite polarity inside schist and granite belt respectively, according to the second profile.

In these models, which were obtained from the profiles trending N-S on the residual map, the iron-bearing formations can be found, whereas an approximately 3.5 km thick was inferred for the central and south-western end of the area. This thickness results can be interpreted in terms of thinning of the crust in the west of the region due to lithospheric stretching, due to upwelling of the upper mantle as a result of isostatic compensation.

The depth of the magnetic bodies interface beyond the Mimbi area seems to correlate with the results of the studies of Paterson et al. (1976) who calculate a three dimensional experimental prismatic model to obtain a body with parameters are  $0.39\mu\text{em}$  concerning susceptibility, with 4.1km of length, have a thickness of about 0.17km and a suggested depth of the top is 0.7 km. In their study, he has identified the body as a pair of body very little spaced, which one has a remanant magnetization (inverse polarity) as those observed at Nkout rocks in Djoum (Ndougsa et al., 2012). The greatest of the apparent magnetic susceptibility and the apparent thickness relatively low has indicated a body presenting a layer shape. He has also attributed the source of observed anomaly at body presenting a lenticular and stratified structure with a high proportion of magnetite under the metasediment.

This paper presents promising results obtained by applying upward continuation method on magnetic data from a metamorphic environment that was probably corrupted by solid mineral. This method that has been used by several authors was unable to attenuate amplitudes with high wavenumber in order to produce wavenumber of interest. The residual anomaly produces after the separation based on this approach provides qualitative enhancements, and with the combination of spectral analysis facilitates improved quantitative analysis in the area under study. Such improvements have the potential to aid in a good mining exploration efforts and solid mineral characterization.

## 7 Conclusion

In this paper, the objective was to propose a 2.5D model derived from the magnetic anomalies, obtained by the upward continuation approach, in order to enhance the accuracy of potential fields data filtering. A 2.5D modelling of residual magnetic field

anomaly is done. This modelling is derived from the combination of spectral analysis based on Fourier transform with the inverse square of distance interpolation, and the upward continuation regional-residual separation approach in order to investigate up to 8.3 km depth in the crust.

The spectral analysis has been used to determine the average depths of the top of the residuals anomalies sources. It is observed that the depths vary between 1.4 km to 2.5 km and between 0.8 km to 3.4 km from the surface of the earth, according to profile P1 and P2 respectively.

The qualitative interpretation of the aeromagnetic data of the study zone enabled us to identify, starting from the magnetic units' map, four target units or zones, of strong magnetic anomalies: including three zones along the axis Mimbi-Nkolembembé-Bissombo and a zone around Messok. These zones present geological indices and geophysics favorable to the iron ore, in particular of itabirites, which, are primarily made up of an iron and silica alternation. Iron is in the form of hematite and of magnetite.

The qualitative magnetic study derived from the application of the upward continuation has permitted to subdivide Mimbi area in four subzones with different particular magnetic responses. Some responses reveal a relative important signature of iron ore deposits, while others highlight the region's fault network.

Modeling 2.5D using the Mag2dc software, with constraint of the depths identified to 1.37 km and 0.77 km by spectral analysis made allow to highlight several magnetic bodies correlated to hematite and the itabirite which one generally finds in the metamorphic formations, in particular schists with oligist, still called iron-bearing mica schists. From the results obtained in this work, it indicates that the various areas of granitic intrusions were observed from the modeling indicating areas of fault lines which matched the proposed faults from the qualitative analysis, although some of the proposed faults turned out to be variations of magnetic susceptibilities of metamorphic rocks.

They are in accordance with the recent studies which have put in evidence a reseau of faults directed SW-NE, and a huge buried magnetite anomaly in the eastern adjacent areas by some authors (Ndougsa et al., 2012; Feumoé et al., 2012).

**ACKNOWLEDGEMENTS:** We are grateful to Professor R. J. Gordon Cooper, School of Earth Sciences, and chairman of the Geophysics group at the University of Witwatersrand for letting us use his 2.5D magnetic modelling and inversion program, and to the reviewers for their valuable comments making the manuscript clear.

## References

- [1] Agocs, W.B., (1951). Least square residual anomaly determination, *Geophysics*, 16, 686-696.
- [2] Anecchione, M.A., Chouteau, M., Keating, P. (2001). Gravity Interpretation of Bedrock Topography: the Case of the Oak Ridges Moraine, Southern Ontario, Canada. *Journal of Applied Geophysics*, 47(1), 63-81
- [3] Basseka C. A., Shandini Y. N., Tadjou J. M. (2011). Subsurface Structural Mapping Using Gravity Data of the northern edge of the Congo Craton, South Cameroon. *Geofizika*, 28(2), 231-244.
- [4] Bhattacharyya, B. K. and Leu Lei-Kuang (1975). Spectral analysis of gravity and magnetic anomalies due to two-dimensional structures. *Geophysics*, 40, 993-1013.

- [5] Bhattacharyya, B.K. and Lei-Kuang Leu (1977). Spectral analysis of gravity and magnetic anomalies due to rectangular prismatic bodies: *Geophysics*, **42** (1), 41-50.
- [6] Billings, S. D., Newsam, G.N., and Beatson, R.K., (2002). Fourier transform of geophysical data using continuous global surfaces. *Geophysics*, **64**, 1378- 1392.
- [7] Blakely, R. J. (1996). Potential theory applied in gravity and magnetic application. *Cambridge University Press*, reprinted edition, Cambridge, 441p.
- [8] Beltrao J.F., Silva JB, and Costa JC. (1991). Robust polynomial tilting for regional gravity fitting. *Geophysics*, **56**, 80-89.
- [9] Boukeke, D.B. (1994). Structures crustales d'Afrique centrale déduite des anomalies gravimétriques et magnétiques: le domaine précambrien de la République Centrafricaine et du Sud-Cameroun, Thèse de Doctorat, université de Paris Sud, 264 p.
- [10] Champetier de Ribes, G., Aubague, M. (1956). Carte géologique de reconnaissance du Cameroun ; feuille N° : NA32 NE-E22. Direction des Mines et de la Géologie du Cameroun.
- [11] Cooper, G. R. J. (2003). Grav2dc. 2.10. An interactive Gravity Modelling program for Microsoft windows, School of Geosciences University of the Witwatersrand, Johannesburg 2050 South Africa.
- [12] Ervin, P.C., (1976). Reduction to the magnetic pole using a fast Fourier series and algorithm. *Computers & Geosciences*, **2**, 211–217.
- [13] Feumoé, A. N., Ndougsa-Mbarga, T., Manguelle-Dicoum, E., and Fairhead, J. D., 2012. Delineation of tectonic lineaments using aeromagnetic data for the south-east Cameroon area. *Geofizika*, **29** (2), 33-50.
- [14] Franke, R. (1982). Scattered Data Interpolation: Test of Some Methods, *Mathematics of Computations*, **33**, 157, 181-200.
- [15] Gentleman, W. M. and Sande, G. (1966). Fast Fourier transformation and profile. *Proc. AFIPS 1966, Fall joint comp. Conf.*, **29**, Spartan books New York, 563-578.
- [16] Gérard, A., and Debeglia, N. (1975). Automatic three-dimensional modeling for the interpretation of gravity or magnetic anomalies. *Geophysics*, **40**, 6, 1014-1034.
- [17] Gérard, A. et Griveau, P. (1972). Interprétation quantitative en gravimétrie ouagnétisme à partir des cartes transformées de gradients vertical. *Geophysical prospecting*, **20**, 2, 459-481.
- [18] Grant, F. S., and Martin, L. (1966). Interpretation of aeromagnetic anomalies by the use of characteristic curves. *Geophysics*, **31**(1), 135-148.
- [19] Guiraudie, Ch., et Gazel, J. (1965). Carte géologique de reconnaissance de la République Fédérale du Cameroun ; feuille N° : NA33 NO 023. Direction des Mines et de la Géologie du Cameroun.
- [20] Henderson, R.G., and Zietz, I. (1949). The Computation of Second Derivatives of Geomagnetic Fields, *Geophysics*, **14**, 508-516.
- [21] Jacobsen, B. H. (1987). A case for upward continuation as a standard separation filter for potential field maps. *Geophysics*, **52**, 1138-1148.
- [22] Mvondo, H., Den Brok, S. W. J. & Mvondo Ondo, J. (2003). Evidence for symmetric extension and exhumation of the Yaoundé nappe (Pan-African fold belt, Cameroon). *Journal of African Earth Sciences*, **36**, 215-231.
- [23] Nabighan, M. N. (1972). The analytic signal of two-dimensional bodies with polygonal cross-section: its properties and use for automated anomaly interpretation. *Geophysics*, **37**(3), 507-517.
- [24] Nnange, J. M., V. Ngako, D. Fairhead and C. J. Ebinger, (2000). Depths to density discontinuities beneath the Adamawa plateau region, Central Africa, from spectral

- analysis of new and existing gravity data. *Journal African. Earth Science*, **40**, 887-901.
- [25] Ndougssa, M.T., Bikoro B. A., Tabod C. T., Sharma K. K. (2013). Filtering of gravity and magnetic anomalies using the finite element approach (fea). *Journal of Indian Geophysical Union*, **17**(2), doi, 2013, in press.
- [26] Ndougssa-Mbarga, T. E., Campos-Enriquez J. O. and Yene-Atangana J. Q. (2007). Gravity anomalies, sub-surface Gravity anomalies, sub-surface structure and oil and gas migration in the Mamfe, Cameroon-Nigeria, sedimentary basin. *Geofisica Internacional*, **46**, 129-139.
- [27] Ndougssa-Mbarga, T., Feumoé, A. N., Manguelle-Dicoum, E., and Fairhead, J. D., 2012. Aeromagnetic data interpretation to locate buried faults in southeast Cameroon. *Geophysics*, **47**(1-2), 49-63.
- [28] Ndougssa M. T., Manguelle-Dicoum E., Tabod C. T., Mbom Abane S. (2003). Modélisation d'anomalies gravimétriques dans la région de Mengueme-Akonolinga (Cameroun). *Sci. Technol. Dev.* **10**(1), 64-74.
- [29] Nedelec, A., Macaudiere, J., Nzenti, J. P. & Barbey, P. (1986). Evolution structurale et métamorphique des schistes de Mbalmayo (Cameroun). Implications sur la structure de la zone mobile Pan-Africaine d'Afrique centrale au contact du craton du Congo. *Comptes Rendus de l'Académie des Sciences Paris*, **303** (2), 1, 75-80.
- [30] Ngnouté, T., Nzenti, J. P., Barbey, P. & Tchoua, F.M. (2000). The Ntui Bétamba high grade gneisses: a northward extension of the Pan-African Yaoundé gneisses in Cameroon. *Journal of African Earth Sciences*, **36**(2), 369-381.
- [31] Njandjock, P.N., Manguelle-Dicoum, E., Ndougssa, M.T., and Tabod, C.T. (2006). Spectral analysis and gravity modelling in the Yagoua, Cameroon, sedimentary basin. *Geofisica Internacional*, **45** (2), 209-215.
- [32] Nzenti, J. P., Barbey, P., Macaudière, J. & Soba, D. (1988): Origin and evolution of the late Precambrian high grade gneisses (Cameroon). *Precambrian Research*, **38**: 91-109.
- [33] Olinga, J. B., Mpesse, J. E., Minyem, D., Ngako, V., Mbarga, T. N. & Ekodeck, G. E (2010). The Awaé–Ayos strike-slip shear zones (southern Cameroon): Geometry, kinematics and significance in the late Pan-African tectonics. *N. Jb. Geol. Paläont. Abh.*, **257**, 1–11.
- [34] Pal, P. C., Khurana, K. K., and Unnikrishnan, P. (1978). Two examples of spectral approach to source depth estimation in gravity and magnetic. *Pageoph*, **117**, 772-783.
- [35] Paterson, Grant and Watson Ltd. (1976). Études aéromagnétiques sur certaines régions de la République Unie du Cameroun. ACDI, Toronto, Canada, 192p.
- [36] Penaye, J., Toteu, S. F., Van Schmus, W. R. & Nzenti, J. P. (1993). U-Pb and Sm-Nd preliminary geochronologic data on the Yaoundé series, Cameroon: reinterpretation of the granulitic rocks as the suture of a collision in the "centrafrican" belt. *Comptes Rendus de l'Académie des Sciences Paris*, **317**, 789-794.
- [37] Prieto, C. (1996). Gravity/ Magnetic signatures of various geologic models An exercise in pattern recognition. *Integrated Geophysics Corporation*, **4**(4), 24 p.
- [38] Spector, A. and Grant, F. S. (1970). Statistical models for interpreting aeromagnetic data. *Geophysics*, **35**(2), 293-302.
- [39] Shandini Y. N.; Tadjou J. M.; Tabod C. T. & Fairhead J. D. (2010). Gravity Data Interpretation in the Northern Edge of the Congo Craton, South Cameroon. *Anuário*

- do Instituto de Geociências– UFRJ*. **33**(1), pp.73-82
- [40] Shuey, R. T., and Pasqual, A. S. (1973). End corrections in magnetic profile interpretation. *Geophysics*, **31**, 362-371.
- [41] Simpson, S.M. (1954). Least-squares polynomial fitting to gravitational data and density plotting by digital computer: *Geophysics*, **19**, 808-811.
- [42] SRK Consulting (UK) Limited, 2011. Report on mineral resource estimate for the Nkout iron ore project, community of Djoum, Cameroon. 128 p.
- [43] Suh C., Cabral A., Ndime E., 2009. Geology and ore fabrics of the Nkout high-grade hematite deposit, southern Cameroon. Society for geology applied to mineral deposits. *Smart Science for Exploration and Mining* P. J. Williams et al. (editors), 558-563.
- [44] Tadjou, J. M., Nouayou R., Kamguia J., Kande H. L. and Mangué-Dicoum E. (2009). Gravity analysis of the boundary between the Congo Craton and the Pan-african belt of Cameroon. *Austrian journal of earth sciences*, **102**, 71-79.
- [45] Talwani, M. (1965). Computation with the help of a digital computer of magnetic anomalies caused by bodies of arbitrary shape. *Geophysics*, **30**, 797-817.
- [46] Telford, W. M., Geldart, L. P., Sheriff, R. E., Keys, D. A. (1990). Applied Geophysics 4th edition, *Cambridge University Press, Cambridge, G.B.*, 860p.
- [47] Toteu, S. F., Van Schmus, W. R., Penaye, J. & Nyobé, J. B. (2004). U- Pb and Sm-Nd evidence for Eburnian and Pan-African high grade metamorphism in cratonic rocks of southern Cameroon. *Precambrian Research*, **67**, 321-347.
- [48] Toteu, S. F., Penaye, J., Deloile, E., Van Schmus, W. R. & Tchameni, R. (2006). Diachronous evolution of volcano-sedimentary basins north of the Congo Craton: Insights from U-Pb ion microprobe dating of zircon from the Poli, Lom and Yaoundé groups (Cameroon). *Journal of African Earth Sciences*, **44**, 428-442.
- [49] Vicat J. P. (1998). Esquisse géologique du Cameroun. Collection GEOCAM, *Presses Universitaire Yaoundé*, pp. 3-11.
- [50] Wong, B.Y. & Laughlin, D.E. (1998). Determination of basic magnetic unit size in CoCrTa/Cr magnetic disk media. *IEEE Transaction on Magnetics*, **34**(1), 293-298.